

# An Efficient Filter Banks Based Multicarrier System in Cognitive Radio Networks

Yun CUI<sup>1,2</sup>, Zhifeng ZHAO<sup>1,2</sup>, Honggang ZHANG<sup>1,2</sup>

<sup>1</sup> York-Zhejiang Lab for Cognitive Radio and Green Communications

<sup>2</sup> Department of Information Science and Electronic Engineering, Zhejiang University

skygon@zju.edu.cn, zhaozf@zju.edu.cn, honggangzhang@zju.edu.cn

**Abstract.** In cognitive radio techniques, OFDM is usually regarded as the physical layer candidate. However, the weaknesses of the OFDM technique, i.e., using plain FFT for spectral analysis, decreased bandwidth efficiency due to CP (cyclic prefix), high out-of-band emission, have been pointed out and the introduction of filter banks based multicarrier (FBMC) system has been advocated by a number of authors. In this paper, we propose an efficient FBMC system for cognitive radio network. At the transmitter, we propose a decimation transform decomposition method to eliminate the unnecessary zero operations. At the receiver, we utilize the analysis filter banks to sense the spectrum bands. In order to conquer the shortages of the traditional filter banks, we propose a multistage analysis filter banks, which can reduce the computational complexity while improve the detection precision when used to sense the spectrum bands. And with an adaptive threshold scheme in the power estimator, the threshold can be kept very close to the noise power, which can increase the detection probability especially in the condition of low SNR.

## Keywords

Cognitive radio, FBMC, transform decomposition, multistage filter banks, adaptive threshold.

## 1. Introduction

Cognitive radio (CR) is a revolutionary intelligence technology which can maximize the utilization of the spectrum band by allowing the second users (SU) access the spectrum holes without causing interference to primary users. During recent years, CR has attracted significant attention of the research community and became a subject of numerous publications including books, special conferences, special issues, tutorials, and research articles [1], [2]. The opportunistic nature of CR systems offers big promises in terms of spectrum usage, but generates a lot of constraints. Basically, such systems must act quickly to access the spectrum and to cease transmission, they must be reliable and robust and they must provide quality of service. And in a licensed band, the main issue is the pro-

tection of the primary user, although the coexistence with other CR users has to be considered as well, for the sake of global efficiency. This means that the primary task in any CR network is to dynamically explore the spectrum holes and determine spectrum band that can be used without causing interference to other users.

The benefits of multicarrier modulation in spectrum sensing context have already been emphasized, such as high spectral resolution, commonality of sensing and communication functions, flexible way of building decision statistics from basic observations within the sensing window and so on. Naturally, OFDM is usually the first choice when talking about multicarrier systems. However, the weaknesses of the OFDM technique, i.e., using plain FFT for spectral analysis, decreased bandwidth efficiency due to CP (cyclic prefix), high out-of-band emission, have been pointed out and the introduction of filter banks based multicarrier (FBMC) system has been advocated by a number of authors [3], [4].

From a transmission perspective, the FBMC technique has the potential to increase the bit rate, due to the reduced guard bands and the absence of the cyclic prefix needed in OFDM. FBMC gives also the possibility to allocate different subcarriers to different non-synchronized users in a spectrally efficient manner. But the out-of-band emission of FBMC is much lower than OFDM. Application of filter banks techniques in spectrum sensing in CR has been studied in references [5], [6]. In this paper, we propose a multistage DFT filter banks (MS-DFTFB) enhanced with an adaptive threshold scheme to sense the spectrum band. It has low computational complexity and high detection precision comparing to the detection method based on traditional DFTFB. And with an adaptive threshold method in our proposed MS-DFTFB, the threshold can be kept very close to the noise power, which can increase the detection probability, especially under the condition of low SNR.

In cognitive radio, the secondary user (SU) using multiple carriers OFDM or FBMC techniques always need to deactivate a number of subcarriers in order to avoid interference to the primary user (PU). This means the OFDM or FBMC based cognitive radio transmitter will have a large number of zero inputs at the IFFT/FFT mod-

ule if there are many subcarriers need to be deactivated as presented in Fig. 1. From a systematic perspective, the IFFT and FFT are the critical modules of the OFDM transceiver, which are also the most computationally intensive blocks in the whole OFDM system. So, an inefficient FFT/IFFT can considerably waste computation power and energy efficiency of the overall cognitive radio system.

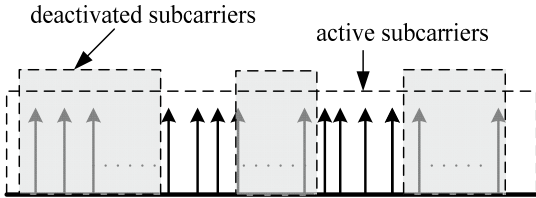


Fig. 1. The usage of a spectrum band for second user.

Up to now, in the literature, several methods have been developed to eliminate or reduce the computation intensity if the input points within an IFFT/FFT module have many zeros or the number of output points acquired is relatively small. These methods are collectively known as FFT pruning [7], [8], [9]. Subsequently, Sorensen and Burrus proposed another method, named as transform decomposition (TD) [10]. In general, TD can be seen as a modified Cooley-Tukey FFT where the DFT is decomposed into two smaller DFTs [11]. In the view point of hardware implementation, TD method is more efficient and flexible than conventional FFT pruning. The FFT pruning or TD has already been applied to the OFDM system instead of standard FFT algorithms in [12] and [13], which both showed significant reduction in arithmetic computation. In this paper, we propose an efficient decimation TD scheme which can reduce the computational complexity comparing with the conventional TD method under the condition of sparse input points.

The rest of this paper is organized as follows: Section 2 describes the decimation TD method and the numeric analysis. Spectrum sensing using our proposed multistage filter banks is presented in section 3.1, followed by an example of two stage filter banks used for wireless microphone detection in IEEE 802.22 WRAN in 3.2. Section 3.3 presents the numeric analysis and simulation results. Section 4 is the adaptive threshold scheme in power estimator followed by the conclusions in section 5.

## 2. Improved Transform Decomposition Method for DFT with Sparse Input Points in FBMC Transmitter

The filter banks system often involves two processes: separation of the frequency components and recombination of the components to recover the original signal. The separation process is known as analysis filter banks and the recombination process is known as synthesis filter banks. Analysis and synthesis filter banks often appear in pairs and satisfy the perfect reconstruction condition which guar-

antees the perfect reconstruction of the signal. We can utilize synthesis filter banks to transmit information in FBMC system as presented in Fig. 2. In order to avoid causing interference to primary users in cognitive radio networks, we need to deactivate some subcarriers as shown in Fig. 1. The deactivation can be realized by loading zeros on the intended subcarriers while others are loaded with modulated complex symbols at the transmitter which is an  $M$  band synthesis filter banks. Therefore, the input points may contain a large number of zero points. By using transform decomposition (TD) method, we can eliminate the unnecessary zero computations, which can help to improve the computational efficiency.

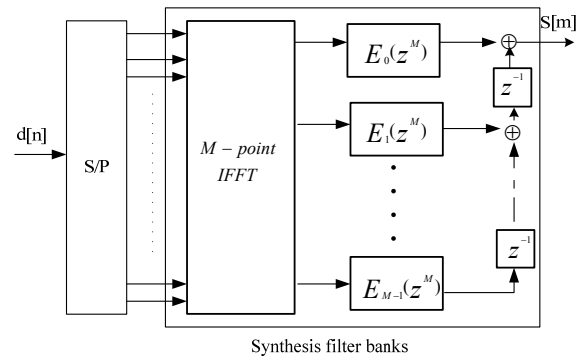


Fig. 2. Basic structure of FBMC transmitter.

### 2.1 Traditional Transform Decomposition

The transform decomposition uses a mixture of a Cooley-Tukey FFT and a computational structure similar to Goertzel’s algorithm [14]. It is shown to be both more efficient and more flexible than pruning. Below, a mathematical derivation of TD for input with few nonzero points is given.

The DFT is defined as

$$X(k) = \sum_{n=0}^{N-1} x(n)W_N^{nk}, \quad k = 0, 1, \dots, N-1 \quad (1)$$

where  $W_N^{nk} = \exp(-j2\pi nk/N)$ . Assume there are  $L$  nonzero inputs and there exist a  $P$ , which is the nearest power-of-two integer larger than  $L$ , divide  $N$  and define  $Q = N/P$ . The index  $n$  can be written as

$$n = Pn_1 + n_2, \quad n_1 = 0, 1, \dots, Q-1, \quad n_2 = 0, 1, \dots, P-1. \quad (2)$$

Similarly, the index  $k$  can be decomposed as

$$k = k_1 + Qk_2, \quad k_1 = 0, 1, \dots, Q-1, \quad k_2 = 0, 1, \dots, P-1. \quad (3)$$

Substituting  $n$  and  $k$  in (1) with (2) and (3), the DFT can be rewritten as

$$\begin{aligned} X(k_1 + Qk_2) &= \sum_{n_2=0}^{P-1} \sum_{n_1=0}^{Q-1} x(Pn_1 + n_2)W_N^{(Pn_1+n_2)(k_1+Qk_2)} = \\ &= \sum_{n_2=0}^{P-1} \left[ \sum_{n_1=0}^{Q-1} x(Pn_1 + n_2)W_N^{(Pn_1+n_2)k_1} \right] W_P^{n_2k_2}. \end{aligned} \quad (4)$$

By taking advantage of equation (5)

$$x_{k_1}(n_2) = \sum_{n_1=0}^{Q-1} x(Pn_1 + n_2) W_N^{k_1(Pn_1+n_2)}, \quad k_1 = 0, 1, \dots, Q-1 \quad (5)$$

we can rewritten equation (4) as (6)

$$X_{k_1}(k_2) = \sum_{n_2=0}^{P-1} x_{k_1}(n_2) W_P^{n_2 k_2}, \quad k_2 = 0, 1, \dots, P-1 \quad (6)$$

where  $X_{k_1}(k_2) = X(k_1 + Qk_2)$ .

For a given  $k_1$ , equation (6) can be recognized as a length  $P$  FFT, which can be computed efficiently using a FFT algorithm. As the  $k_1$  can range from 0 to  $Q-1$ , there are  $Q$  length  $P$  FFT operations. For each length  $P$  FFT, we need to acquire  $x_{k_1}(n_2)$  by using (5). Since there are  $L$  nonzero input points, the multiplications used by (5) will be  $L$  at a given  $k_1$  when  $n_2$  traverses from 0 to  $P-1$ . When  $k_1 = 0$ , then  $W_N^{k_1(Pn_1+n_2)} = 0$ , equation (5) exists only additions. Therefore, the total number of multiplications cost by (5) will be  $(Q-1)L$  when  $k_1$  ranges from 0 to  $Q-1$ . The total number of multiplications used by TD is given as

$$Num_{TD} = Q \frac{P}{2} \log_2 P + (Q-1)L. \quad (7)$$

## 2.2 Proposed Decimation Transform Decomposition Method

Thereinafter, we propose an efficient transform decomposition method which can reduce the computational complexity further more comparing to the traditional TD method. We denote this method as decimation transform decomposition (DTD), because the proposed method needs to decimate the input  $x(n)$  into two separate sets. The method DTD is somewhat like the way from a DFT to decimation-in-time FFT (DIT-FFT). We first divide the input points  $x(n)$  into two groups, one is the set with even index  $n$  and the other is the set with odd  $n$ , which is described in (8)

$$x_1(r) = x(2r), \quad x_2 = x(2r+1), \quad r = 0, 1, \dots, \frac{N}{2} - 1. \quad (8)$$

Then equation (1) can be rewritten as

$$X(k) = \sum_{r=0}^{N/2-1} x_1(r) W_{N/2}^{rk} + W_N^k \sum_{r=0}^{N/2-1} x_2(r) W_{N/2}^{rk}, \quad (9)$$

which divides a  $N$  point DFT into two  $N/2$  point DFT. Because of the symmetry of  $W_{N/2}^{rk}$ , which is  $W_{N/2}^{rk} = W_{N/2}^{r(k+N/2)}$ ,  $X(k)$  can be acquired according to the  $X_1(k)$  and  $X_2(k)$ , as equation (10) shows:

$$X(k) = X_1(k) + W_N^k X_2(k),$$

$$X\left(k + \frac{N}{2}\right) = X_1(k) - W_N^k X_2(k), \quad k = 0, 1, \dots, \frac{N}{2} - 1 \quad (10)$$

where  $X_1(k) = \sum_{r=0}^{N/2-1} x_1(r) W_{N/2}^{rk}$ , and  $X_2(k) = \sum_{r=0}^{N/2-1} x_2(r) W_{N/2}^{rk}$ .

Instead of using TD on  $X(k)$ , we perform TD on  $X_1(k)$  and  $X_2(k)$ . Then we use (9) to get  $X(k)$ . Assume there are  $L$  nonzero inputs and  $L_1$  nonzero inputs are in the even set  $x_1(r)$  while  $L_2$  (which is also  $L - L_1$ ) in the odd set  $x_2(r)$ . The TD on  $X_1(k)$  and  $X_2(k)$  is the same as (4) and (5), respectively. We assume  $P_1$  ( $P_2$ ) is the nearest power-of-two integer larger than  $L_1$  ( $L_2$ ), and  $Q_1 = N/(2P_1)$ ,  $Q_2 = N/(2P_2)$ . The number of multiplications needed for our proposed DTD method is given by (11)

$$Num_{DTD} = Q_1 \frac{P_1}{2} \log_2 P_1 + (Q_1 - 1)L_1 + Q_2 \frac{P_2}{2} \log_2 P_2 + (Q_2 - 1)L_2 + \frac{N}{2}$$

$$= \frac{N}{4} \log_2(P_1 P_2) + (Q_1 - 1)L_1 + (Q_2 - 1)L_2 + \frac{N}{2}. \quad (11)$$

The component  $N/2$  in (10) is the number of multiplications that equation (9) needs to compose  $X_1(k)$  and  $X_2(k)$  into  $X(k)$ . Fig. 3 presents the block diagram for the proposed novel TD method. The input  $x(n)$  is divided into two sets as mentioned above, one is  $x_1(r)$  and another is  $x_2(r)$ . Then the conventional TD is carried out on  $x_1(r)$  and  $x_2(r)$  separately. The output mapping process is used to get the  $X_1(k)$  and  $X_2(k)$  in natural order by utilizing (3). The final  $X(k)$  we need is then produced by butterfly operation as equation (9) shows. It is the combination of conventional TD and partial DIT-FFT which can achieve the computational efficiency comparing with the TD.

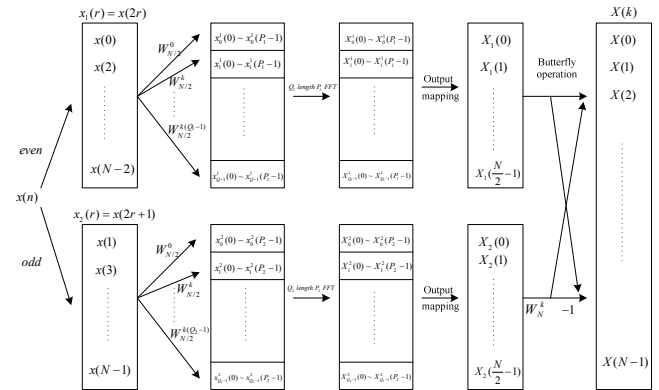


Fig. 3. Block diagram of proposed efficient TD method for sparse input points DFT.

## 2.3 Numerical Results and Computational Complexity Analysis

In this section, we discuss the computational complexity of conventional TD and our proposed DTD method in different conditions. As mentioned above, the computational complexity of conventional TD (CTD) is given by equation (7), while the proposed DTD's complexity is given by (11). Fig. 4 presents the number of multiplications CTR2-FFT, conventional TD and our proposed DTD needs under the hypothesis that the nonzero input points are all in one single set. If the nonzero ratio is bigger than 0.5, then we assume the  $N/2$  nonzero input points are in one set and the remains nonzero input points in another set. In Fig. 4,

when the nonzero input points is less than  $N/2$ , which is 512 exactly, we assume the nonzero points are all in one set, the odd set  $x_2(r)$ , for example. In the case the nonzero ratio is bigger than 0.5, we assume there are  $N/2$  points in one set, and the remains are in another set. When the nonzero ratio is bigger than 0.5, from Fig. 4, we can see that the number of complex multiplications of CTD is equal to CTR2-FFT. While the nonzero ratio is about 0.75 the number of multiplications of DTD and CTR2-FFT are equal. When the nonzero ratio is less than 0.5 in Fig. 4, the number of complex multiplications DTD needs is much less than CTD needs. This is because there is one set do not need to be operated when the nonzero ratio is less than 0.5.

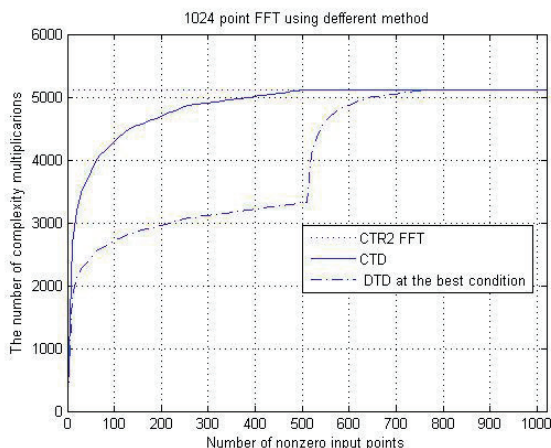


Fig. 4. The number of complex multiplications that CTR2-FFT, conventional TD (CTD) and our proposed method (DTD) need under the hypothesis that mentioned above.

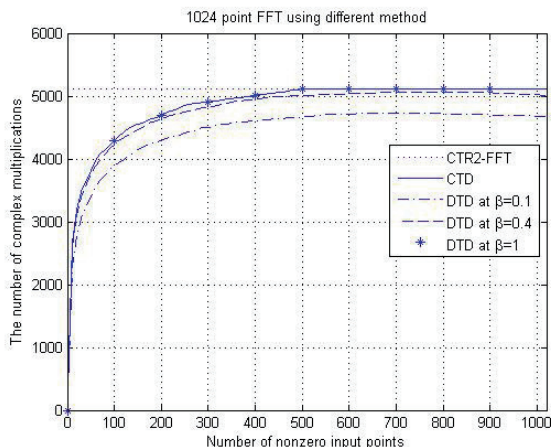


Fig. 5. The number of complex multiplications that DTD needs at different distribution degrees.

When the nonzero input points are arbitrary distributing in the two sets, the result will be different from Fig. 5, obviously. We use the distribution degree to denote the randomness of the nonzero input points as  $\beta = L_1/L_2$ ,  $L_1$  is the number of nonzero points in the even set  $x_1(r)$  while  $L_2$  is the number in set  $x_2(r)$ . Obviously, Fig. 4 is the scenario that  $\beta = 0$ . Fig. 5 presents the number of multiplications

that CTD and DTD need at different distribution degrees. From Fig. 5, we can see that the gap between the CTD curve and DTD curve is becoming more and more narrower as the increasing of distribution degree  $\beta$ . The number of multiplications that CTD and DTD need are almost equal when  $\beta = 1$ . This means that when the nonzero input points are uniformly distributing, the computational complexity of DTD and CTD are almost the same.

### 3. Multistage Filter Banks for Spectrum Sensing in Cognitive Radio Networks

The receiver of the FBMC system is an analysis filter banks as shown in Fig. 6. And we can utilize the analysis filter banks (AFB) to sense the spectrum band. In Fig. 6, the analysis filter banks utilize the polyphase structure and IFFT. We name this AFB as DFT filter banks (DFTFB). A traditional M band DFTFB divides the spectrum band into  $M$  subbands and by calculating the energy of each subband we can know whether this subband is occupied or not. The detection precision is directly affected by the parameter  $M$ , which is the number of subbands of the M band filter banks. If we want higher detection precision, we need to increase the value of  $M$ , which will cause the rapid increasing of computational complexity.

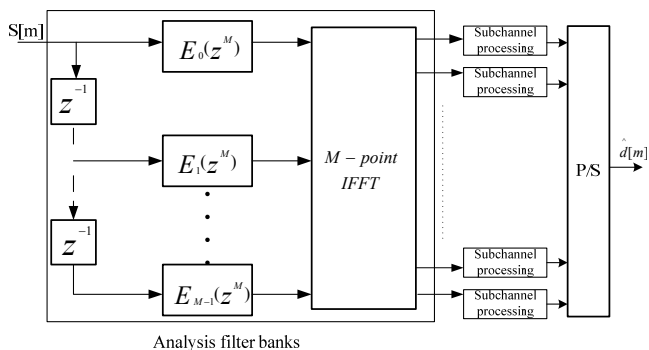


Fig. 6. Basic structure of FBMC receiver.

#### 3.1 Proposed Multistage Analysis Filter Banks

In order to reduce the computational complexity while improve the detection precision, we divide the traditional DFTFB into  $N$  stages.

*Stage 1:* We first use an  $M_1$  band DFTFB to sense the spectrum that we interest in. If there are narrow band users existing in the spectrum band and the detection result is not precise enough, we carry out *stage 2*.

*Stage 2:* We use an  $M_2$  band DFTFB to detect the narrow band user we interest in (we use  $x_m(n)$  to denote our target signal below) based on the result of stage 1. We divide the subband which has detected  $x_m(n)$  in stage 1 into

$M_2$  subbands. These  $M_2$  subbands can build up an  $M_2$  DFTFB, which has much narrower subband comparing with  $M_1$  DFTFB. If the narrow band signal spans two or more subbands, for example SU2, as presented in Fig. 7, we divide these adjacent subbands into  $M_2$  subbands and then build up an  $M_2$  band DFTFB. If the detection precision is still not good enough, we can carry out *stage 3*, *stage 4*, ... *stage N*, until the detection precision achieves our requirement. The process is just as same as stage 1 to stage 2.

Before we carry out our analysis on MS-DFTFB, we need to make some useful definitions. Assume the bandwidth of the spectrum we want to sense is  $W_0$  and the frequency of the spectrum band ranges from 0 to  $W_0$ . (In fact, by using a down conversion, we can change any spectrum band into base band.) We define  $S_i$  as the number of subbands that  $x_{in}(n)$  spans in the  $M_i$  band DFTFB of stage  $i$ ,  $i=1,2,\dots,N-1$ . In Fig. 7, for example,  $S_1=1$  for SU1 and  $S_1=2$  for SU2.  $N$  is the number of total stages of MS-DFTFB. Obviously, the bandwidth of subband in  $M_1$  band DFTFB is  $W_0/M_1$ . The bandwidth of the subband in the  $i^{\text{th}}$  stage's  $M_i$  band DFTFB ( $W_{sub}^i$ ) is given by

$$W_{sub}^i = S_{i-1}W_{i-1} / (M_{i-1}M_i), \quad i = 2,3,\dots,N. \quad (12)$$

The center frequency of  $x_{in}(n)$  ( $f_{cx}$ ) is decided by the subbands that detected  $x_{in}(n)$  in the  $i^{\text{th}}$  stage, which are assumed  $k^{\text{th}}$  to the  $(k+S_i-1)^{\text{th}}$  subbands of the  $M_i$  band DFTFB, as presented in equation (13)

$$f_{cx}^i = f_k + \frac{W_i}{2\pi M_i} \cdot \frac{S_i}{2}, \quad i = 1,2,\dots,N \quad (13)$$

where  $f_k$  is the start frequency of the  $k^{\text{th}}$  subband.

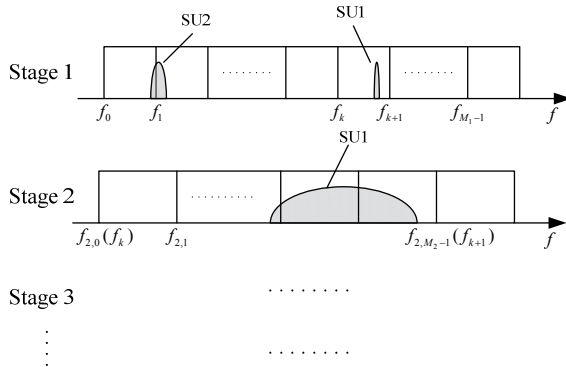


**Fig. 7.** The scheme of proposed multistage DFTFB.

The detailed method of dividing the interested subband(s) of  $M_{i-1}$  ( $i > 1$ ) band DFTFB into  $M_i$  subbands and build up an  $M_i$  band DFTFB is as following ( $i^{\text{th}}$  stage): We assume the lowest index of the subbands that have detected  $x_{in}(n)$  is  $k$ , which means the  $x_{in}(n)$  spans from the  $k^{\text{th}}$  to the  $(k+S_{i-1}-1)^{\text{th}}$  subbands of the  $M_{i-1}$  band DFTFB. Then we divide these  $S_{i-1}$  subbands into  $M_i$  subbands and build up an  $M_i$  band DFTFB. We assume the types of the prototype filters of  $M_i$   $i=1,2,\dots,N$  band DFTFB are same except the bandwidth. The initial start frequency of  $M_i$  band DFTFB

is 0. In order to sense the  $k^{\text{th}}$  to  $(k+S_{i-1}-1)^{\text{th}}$  subbands of the  $M_{i-1}$  band DFTFB, we need to modulate the center frequency of  $M_i$  band DFTFB onto the center frequency of those subbands of  $M_{i-1}$  band DFTFB. This can be realized by multiplying a modulation component after each poly-phase component  $E_i(z)$ ,  $i=0,1,\dots,M_i-1$  in Fig. 6. In the  $i^{\text{th}}$  stage, the modulation component ( $C_m^i$ ) is defined as  $C_m^i = \exp(j2\pi f_{M_{i-1}} + j(2k-1)W_{sub}^{i-1}/2)$ , where  $f_{M_{i-1}}$  is the start frequency of the filter banks in the  $(i-1)^{\text{th}}$  stage.

The whole structure of our proposed scheme is presented in Fig. 8(a). There are  $N$  stages and each stage (except stage 1) has two input flows. One is the detection information, which is used to set the modulation component. The other is the SU signal ( $x_{in}(n)$ ) we want to detect from the antenna. Fig. 8(b) is the structure of the  $M_i$  band DFTFB in the  $i^{\text{th}}$  stage. In Fig. 8(b),  $C_m = \exp(j2\pi f_{M_{i-1}} + j(2k-1)W_{sub}^{i-1}/2)$  is the modulation component of the  $i^{\text{th}}$  stage.

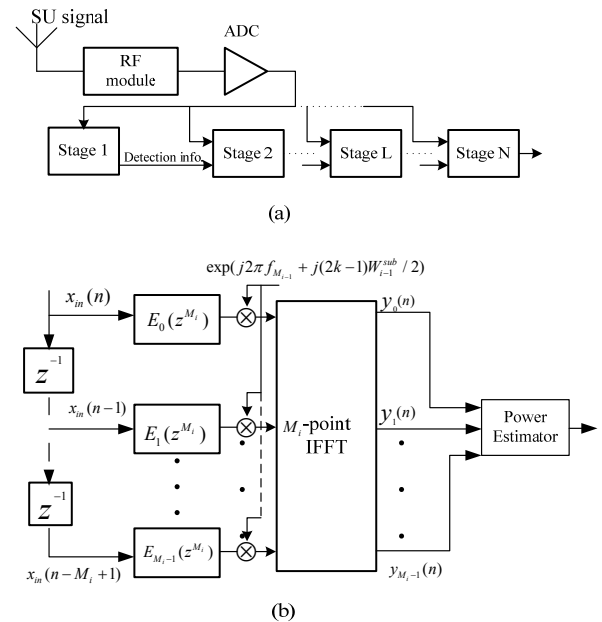


**Fig. 8.** (a) Brief structure of the proposed multistage DFT filter banks. (b) Structure of DFT filter banks with modulation component in stage  $L$ .

### 3.2 An Example: Wireless Microphone Detection in IEEE 802.22 WRAN Using Proposed Multistage AFB

In 802.22 WRAN, at any time when there is wireless microphone (WM) appearing in TV channel, the whole channel of 6 MHz bandwidth should be evacuated immediately for interference avoidance. In order to avoid interference to WM when other users using the adjacent TV channel, we need to know the precise location of WM. Usually, the bandwidth of WM is 200 kHz or less. Traditional DFTFB divide the whole 6 MHz TV channel into 30 or more subbands. By detecting the energy of each subband,

we can locate the occupied frequency of WM. In this section, considering the complexity of hardware implementation, we choose a two stage DFTDB (TS-DFTFB) as mentioned in 3.1 to sense the 6 MHz TV channel. The whole architecture of two stage filter banks is presented in Fig. 9.

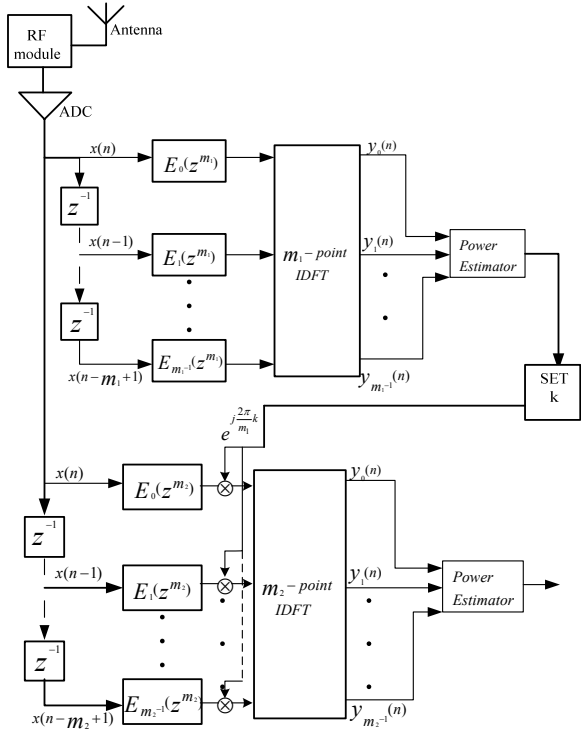


Fig. 9. Architecture of the two stage filter banks.

We use a RF module followed by an ADC to sample the receiving WM signal. A rough detection is carried out by the  $m_1$  band DFTFB at the stage 1, which estimates the output power of each subband. Then the modulation component  $k$  is set up by the “SET  $k$ ” module according to the rough detection result. A precise result will be obtained during the second stage that relies on much narrower subband to detect the WM with increased resolution. The power estimator module is used to calculate the power of each subband and adaptively setting the threshold. More detail of the power estimator module will be described in section 4. We assume the WM users are slowly changing so that there is no need to save the data from ADC into a buffer for precise detection in stage 2. In addition, there is no need to further divide the  $m_2$  band DFTFB into much narrower DFTFB like stage 1 to stage 2 in this paper, because we consider that the detection result is relatively precise enough for the WM, comparing with the 6 MHz TV channel, and the hardware implementation complexity will increase if we divide the DFTFB into 3 or more stages.

### 3.3 Numerical Analysis and Simulation Results

As multiplication is the most complex operation in filtering, we use the number of complex multiplication to

estimate the computational complexity. In this section, we do not consider the complexity of the power estimator module, because the adaptive threshold scheme is periodic and in a relevant long time, we can use the same threshold and do not need to change it. Corresponding to the traditional DFTFB (t-DFTFB) mentioned above, the number of complex multiplication is given by

$$n_{t-DFTFB} = l(h_0(n)) + \frac{M}{2} \log_2 M \tag{14}$$

where  $l(h_0(n))$  is the points of the prototype filter,  $M$  is the number of total subbands. In (14),  $M$  is a power-of-two integer.

In comparison, the number of complex multiplication of the TS-DFTFB is given by:

$$n_{TS-DFTFB} = l(h_{10}(n)) + \frac{m_1}{2} \log_2(m_1) + 2l(h_{20}(n)) + \frac{m_2}{2} \log_2(m_2) \tag{15}$$

where  $l(h_{i0}(n))$ ,  $i = 1, 2$ , is the points of prototype filters of the  $m_i$ ,  $i = 1, 2$  band DFTFB. Similar to equation (14),  $m_1$  and  $m_2$  are both power-of-two integers.

The number of multiplications of the  $m_2$  band DFTFB is adding another  $l(h_{20}(n))$  compared with  $m_1$  band DFTFB in (15). This is because the modulation at the stage 2 costs additional  $l(h_{20}(n))$  complex multiplications. The total points of  $\sum_{l=0}^{M-1} E_l(z^M)$  is just the length of the prototype filter in Fig. 9, and the number of complex multiplications cost on modulating  $m_2$  band DFTFB to the center frequency of WM that we get in stage 1 is just  $l(h_{20}(n))$ . In order to avoid aliasing in the  $M$  band DFTFB, it is necessary to ensure the points of prototype filter be bigger than  $M$ . In this paper, we choose the length of prototype filter  $\gamma$  times as the total bands of DFTFB, namely  $l(h_0(n)) = \gamma M$ ,  $\gamma \geq 1$ .

When we use traditional DFTFB or TS-DFTFB to detect the WM, if the WM spans two or more adjacent filters, we have to choose the center frequency of those filters as the WM’s center frequency. Obviously, the bigger the value of  $M$  or  $m_1 \times m_2$  is, the smaller the detection error will be. Fig. 10(a) presents the simulation results of detection error of the 32 band traditional DFTFB and the TS-DFTFB with coefficients of  $m_1 = 8$ ,  $m_2 = 4$ . A sequence of wireless microphones with random center frequencies is used to carry out our simulation. We assume that whenever there is a WM appearing in a specific TV channel, it can be detected immediately. From Fig. 10(a), we can observe that, the detection precision of traditional DFTFB and TS-DFTFB is almost same when  $M = m_1 \times m_2$ . Fig. 10 (b) presents the number of complex multiplications that traditional DFTFB and TS-DFTFB needed when the value of  $M$  and  $m_1 \times m_2$  is equal. We can find that, when the detection precision is same, the number of multiplications of TS-DFTFB is smaller than traditional DFTFB.

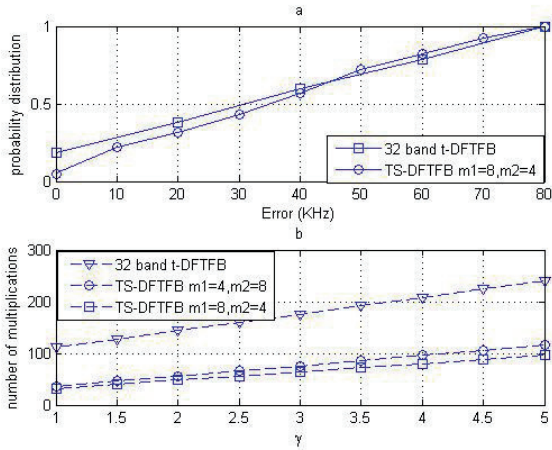


Fig. 10. (a) Detection error of 32 band t-DFTFB and TS-DFTFB. (b) Number of multiplications of 32 band t-DFTFB and TS-DFTFB.

### 4. Power Estimator with Adaptive Threshold

In this paper, we use an adaptive threshold algorithm to determine whether there is WM in TV channel in section 3.2 (it obviously can be used in other situation of spectrum sensing), which is the AT module in Fig. 11. The main idea is coming from reference [15], but we made some modification in our paper. The architecture in dashed rectangle in Fig.11 is the detailed structure of power estimator module. The output of each subband of the  $m$  band DFTFB  $\gamma_i(n)$ ,  $i = 0, 1, \dots, m-1$  is firstly operated by  $|\gamma_i(n)|^2/N$ , which is in order to calculate the power of each subband. Then the subband power comparison (SPC) module is used to compare the power of each subband with the threshold set by the adaptive threshold (AT) module. Whether there is WM in TV channel as well as the average noise power  $p_n$  can be acquired in this module. (If several continuous subbands have bigger output power than the threshold, the SPC module will decide these subbands are occupied by WM, and the average power of noise  $p_n$  is the average power of the remaining subbands.) The WM detection information is just the output of our proposed power estimator and the average noise power  $p_n$  is sent to the adaptive threshold (AT) module in order to get the next period's threshold value.

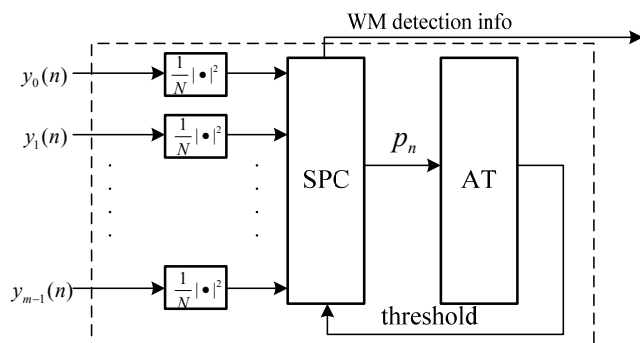


Fig. 11. Detailed power estimator module in Fig. 9.

The method [15] we choose to adaptively set the threshold is as following:

$$p_{th}(i) = p_{th0} + \beta(i) \tag{16}$$

where  $p_{th}(i)$  is the threshold in the  $i^{th}$  period that set by AT, and  $p_{th0}$  can be adaptively set according to the spectrum environment and the white Guasson noise (WGN). In order to reduce false alarm,  $p_{th0}$  should be big enough to ensure the threshold is bigger than the noise. While in the other hand,  $p_{th0}$  should be properly set to ensure the threshold is smaller than the signal, which can reduce the probability of leakage alarm. Another component  $\beta(i)$  is presented in (17), where the modification is made in.

$$\beta(i) = \beta(i-1) \frac{\alpha}{1+\alpha} + p_n(i-1) \frac{C_p}{1+\alpha}, \quad i = 2, 3, \dots, m \tag{17}$$

where  $p_n(i-1)$  is the average noise power in the  $(i-1)^{th}$  period (in reference [15],  $p_n(i)$  will be instead of  $p_n(i-1)$ ),  $\alpha$  and  $C_p$  are two adaptive parameters.  $\alpha$  mainly affects the tendency of  $\beta(i)$  and  $C_p$  can control the degree that  $\beta(i)$  affected by the noise. We usually set  $C_p$  to 1 if the noise is varying very slowly. The average noise power  $p_n(i-1)$  can be acquired according to the result of the  $(i-1)^{th}$  period's detection result and can be used to mend the threshold in the  $i^{th}$  period. This is the main motivation that we use  $p_n(i-1)$  instead of  $p_n(i)$  in our paper.

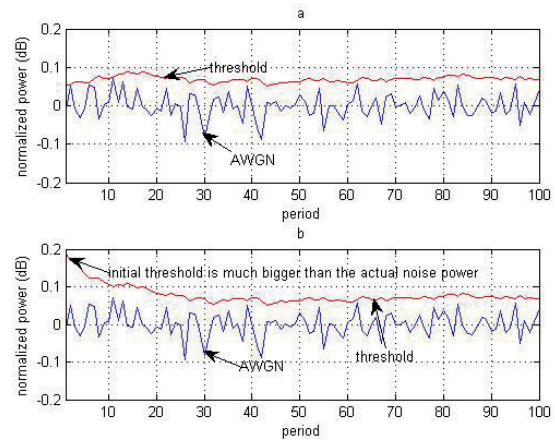


Fig. 12. (a) Threshold and AWGN curves, where the initial threshold is varying to the actual noise power. (b) Threshold and AWGN curves, where the initial threshold is much bigger than the noise power. (The values of adaptive parameters are  $\alpha = 6, C_p = 1.$ )

We can use the threshold  $p_{th}(i)$  to determine whether there is WM in TV channel by comparing the power of each subband with the threshold in the  $i^{th}$  period. The value of threshold exported to SPC module from AT module will maintain unchanging in the whole period. This means that we should set the threshold again after a period according to the spectrum environment, which is exactly the average noise power  $p_n$  in this paper. When we use the adaptive threshold method in (16) and (17), we need an initial threshold  $p_{th}(1)$ , which is an empirical value. Even if the initial threshold we set is bigger or smaller than the actual

noise power, the following thresholds will be adaptively amended to the actual noise power after several periods, just as presented in Fig. 12. We can see that the adaptive threshold curve is much smoother than the noise power curve from Fig. 12 (a). And with a proper value of  $p_{th0}$ , we can ensure the threshold almost always bigger than the noise power in order to reduce the probability of false alarm. Fig. 12 (b) is the situation that initial threshold  $p_{th}(1)$  is much bigger than the actual noise power. We can find that after several periods, the threshold is very close to the noise power just as in Fig. 12 (a).

## 5. Conclusions

In this paper, we propose an efficient FBMC system for cognitive radio networks. At the transmitter, we propose a decimation transform decomposition method to eliminate the unnecessary zero operations. At the receiver, we utilize the analysis filter banks to sense the spectrum bands. In order to conquer the shortages of the traditional filter banks, we propose a multistage filter banks, which can reduce the computational complexity while improve the detection precision when used to sense the spectrum bands. This scheme has been analyzed and tested through simulations on wireless microphone detection in IEEE 802.22 WRAN. The simulation results also demonstrate our theoretical analysis. Besides, we also use an adaptive threshold scheme to determine whether there is primary user in a spectrum band. Simulation results show that the adaptive method can keep the threshold close to the noise power, even if the initial threshold is much bigger or smaller than the actual noise power, which can increase the detection probability especially in low SNR.

## Acknowledgement

This paper is supported by the Key Project of the Education Department of Zhejiang Province (No. 20070247), the Key Project of the Office of Science and Technology of Zhejiang Province (No. 2008C01051-3), and the Key Project of the Ministry of Industry and Information Technology of China ("Research on Broadband Wireless Access Systems Architecture and Framework for Supporting Broadcasting Services" No.2009ZX03005-004).

## References

- [1] MITOLA, J., MAGUIRE, G. Q. Cognitive radios: making software radios more personal. *IEEE Personal Communications*, Aug. 1999, vol. 6, no. 4, p. 13-18.
- [2] HAYKIN, S. Cognitive radio: brain-empowered wireless communications. *IEEE Journal of Selected Areas in Communications*, Feb. 2005, vol. 23, no. 2, p.201-220.

- [3] ZHANG, Q., KOKKELER, A. B. J, SMIT, G. J.M. An oversampled filter bank multicarrier system for Cognitive Radio. In *IEEE Personal, Indoor and Mobile Radio Communications (PIMRC)*. Cannes (France), 2008, p. 1-5.
- [4] WALDHAUSER, D. S., BALTAR, L. G., NOSSEK, J. A. Comparison of filter bank based multicarrier systems with OFDM. In *IEEE Asia Pacific Conference on Circuits and Systems (APCCAS)*. Singapore, 2006, p. 976-979.
- [5] BEHROUZ, F. B. Filter bank spectrum sensing for cognitive radios. *IEEE Transactions on Signal Processing*, May 2008, vol. 56, p. 1801-1811.
- [6] SHEIKH, F., BING, B. Cognitive spectrum sensing and detection using polyphase DFT filter banks. In *Proceedings of IEEE Consumer Communications and Networking Conference (CCNC 08)*. Las Vegas (USA), Jan. 2008, p. 973-977.
- [7] MARKEL, J. FFT pruning. *IEEE Transactions on Audio and Electroacoustics*, 1971, vol. 19, p. 305-311.
- [8] SKINNER, D. Pruning the decimation in time FFT algorithm. *IEEE Transactions on Acoustics, Speech and Signal Processing*, 1976, vol. 24, p. 193-194.
- [9] ALVES, R. G., OSORIO, P. L., SWAMY, M. N. S. General FFT pruning algorithm. In *Proceedings of the 43rd IEEE Midwest Symposium on Circuits and Systems*. Lansing (MI, USA), 2000, vol. 3, p. 1192-1195.
- [10] SORENSEN, H. V., BURRUS, C. S. Efficient computation of the DFT with only a subset of input or output points. *IEEE Transactions on Signal Processing*, 1993, vol. 41, p. 1184-1200.
- [11] COOLEY, J. W., TUKEY, J. W. An algorithm for machine computation of complex Fourier series. *Math. Comput.*, Apr. 1965, vol. 19, p. 297-301.
- [12] SHOUSHENG HE, TORKELSON, M. Computing partial DFT for comb spectrum evaluation. *IEEE Signal Processing Letters*, June 1996.
- [13] ZHANG, Q., KOKKELER, A. B. J, SMIT, G. J.M. An efficient FFT for OFDM based cognitive radio on a reconfigurable architecture. In *IEEE International Conference on Communication*. Glasgow (UK), June 2007.
- [14] GOERTZEL, G. An algorithm for the evaluation of finite trigonometric series. Jan. 1958, *Amer. Math. Monthly*, vol. 65, p. 34-35.
- [15] MINJIAN ZHAO, Study on multi-band, multi-rate, multi-mode software radio receivers. *Ph.D Thesis*, Zhejiang University, 2003.

## About Authors...

**Yun CUI** is a Master student at the Department of Information Science and Electronic Engineering, Zhejiang University, China. His research interests are cognitive radio and multicarrier systems, mainly focusing on filter banks based multicarrier system in cognitive radio networks. In the area of spectrum sensing based on filter banks techniques, he has one patent application, and also has published several papers.

**Zhifeng ZHAO** is an Associate Professor at the Department of Information Science and Electronic Engineering, Zhejiang University, China. He received the Ph.D. degree in Communication and Information System from the PLA University of Science and Technology, Nanjing, China, in

2002. Prior to that, he received the Master degree of Communication and Information System in 1999 and Bachelor degree of Computer Science in 1996, from the PLA University of Science and Technology, respectively. From September 2002 to December 2004, he acted as a postdoctoral researcher at the Zhejiang University. From January 2005 to August 2006, he acted as a senior researcher at the PLA University of Science and Technology, Nanjing, China, where he performed research and development on advanced energy-efficient wireless router, Ad Hoc network simulator and cognitive mesh networking test-bed. His research area includes cognitive radio, wireless multi-hop networks (Ad Hoc, Mesh, WSN, etc.), wireless multimedia network and Green Communications.

**Honggang ZHANG** is a Full Professor at the Department of Information Science and Electronic Engineering, Zhejiang University, China. He received the Ph.D. degree in

Electrical Engineering from Kagoshima University, Japan, in 1999. From October 1999 to March 2002, he was with the Shin-Kawasaki Research Center, Telecommunications Advancement Organization (TAO) of Japan, as a TAO Research Fellow. From April 2002 to November 2002, he joined the TOYOTA IT Center. From December 2002 to August 2004, he has been with the UWB (Ultra-Wideband) Research Consortium, at the Communications Research Laboratory (CRL) and National Institute of Information and Communications Technology (NICT) of Japan. From September 2004 to February 2008, he has been with CREATE-NET (Trento, Italy) where he led its wireless teams in exploring cognitive radio and its integration with Ultra-Wideband technologies for open-spectrum wireless communications and networks evolution. His research interests are in Ultra-Wideband wireless communications, cognitive radio, broadband networks integration, and Green Communications.